Published in final edited form as:
Mol Cancer Ther. 2009 January ; 8(1): 178–184. doi:10.1158/1535-7163.MCT-08-0643.

CXCR4-gp120-IIIB interactions induce caspase-mediated apoptosis of prostate cancer cells and inhibit tumor growth

Shailesh Singh[1], **Vincent C. Bond**[2], **Michael Powell**[2], **Udai P. Singh**[3], **Harvey L. Bumpers**[2], **William E. Grizzle**[4], and **James W. Lillard Jr.**[1,2]

[1]Department of Microbiology and Immunology, James Graham Brown Cancer Center, University of Louisville School of Medicine, Louisville, Kentucky

[2]Department of Microbiology, Biochemistry, and Immunology, Morehouse School of Medicine, Atlanta, Georgia

[3]Department of Pathology, Microbiology and Immunology, University of South Carolina School of Medicine, Columbia, South Carolina

[4]Department of Pathology, University of Alabama at Birmingham Comprehensive Cancer Center, Birmingham, Alabama

Abstract

CXC chemokine receptor 4 (CXCR4) has been implicated in prostate cancer metastasis and this receptor also acts as a coreceptor for HIV-1 120-kDa glycoprotein variant IIIB (gp120-IIIB). The interaction between CXCR4 and gp120-IIIB has been shown to mediate apoptosis of both immune and endothelial cells. In this study, we have examined the effects of gp120-IIIB on hormone-refractory prostate cancer cells (PC3 and DU145) *in vitro* and tumor growth *in vivo*. Normal prostatic epithelial (PrEC) and prostate cancer cell lines were treated with gp120-IIIB with or without anti-CXCR4 antibody. Caspase expression was evaluated by real-time PCR and active caspase assays. Apoptosis was determined by flow cytometry. gp120-IIIB treatment correlated with active caspase-3 and -9 expression and apoptosis of prostate cancer cells but not PrEC cells. This effect was significantly inhibited after CXCR4 blockade. PC3 and DU145 tumor-bearing mice received intraperitoneal injections of gp120-IIIB and controls received bovine serum albumin in PBS. PC3 and DU145 tumor sizes were measured over time and excised tumors were evaluated for CD44, CD34, lymphatic endothelial cell marker LYVE-1, active caspase-3, and active caspase-9 expression by immunohistochemistry. The tumor size in mice receiving gp120-IIIB was significantly smaller than compared with tumors in control mice. This regression was associated with significant decreases in CD44, CD34, and LYVE-1 and increases in active caspase-3 and -9 expression. These results suggest that gp120-IIIB induced apoptosis in prostate cancer cells and reduced tumor-associated lymphoendothelial cells.

Introduction

Despite recent advancements in the treatment and management of prostate cancer, it still remains the most common malignancy and second leading cause of cancer-related deaths

Requests for reprints: James W. Lillard, Jr., Department of Microbiology and Immunology, James Graham Brown Cancer Center, University of Louisville School of Medicine, 580 South Preston Street, Baxter II Room 304, Louisville, KY 40202. Phone: 502-852-2174; Fax: 502-852-3842. james.lillard@louisville.edu.

Disclosure of Potential Conflicts of Interest
No potential conflicts of interest were disclosed.

among men in the United States. The main treatment strategy for advanced prostate cancer involves androgen ablation. Unfortunately, this therapy eventually fails and many patients frequently develop metastatic disease. New agents that would prevent and/or inhibit hormone-refractory prostate cancer progression are needed.

CXC chemokine receptor 4 (CXCR4) and its ligand CXCL12 have been implicated in prostate cancer (1, 2) and in other malignancies (3–6). CXCR4-CXCL12 interaction has been proposed to play a significant role in prostate cancer cell homing (1, 7, 8) and other tumor cell types to several anatomic sites (4–6, 9). These studies suggest that the development of CXCR4 antagonists would be useful in inhibiting cancer progression and metastasis. Although small-molecule inhibitors (plerixafor, maraviroc, etc.) of chemokine receptors show promise, these hydrophobic molecules may prove difficult to deliver and might be associated with inferior clinical performance and toxicities (10, 11). CXCR4 also acts as a coreceptor for certain isolates of HIV-1 (12, 13). In addition to infection, HIV-1 gp120 variants have been shown to mediate apoptosis of several cell types in a CXCR4-dependent fashion (14, 15).

Metastasis via blood vessels is well recognized for many tumors and correlates with cancer progression (16). However, tumor growth and metastasis can be supported by both vascular and lymphatic endothelia (17). The number and size of lymphatics in and around tumors are an important determinant for metastasis (18–20). In light of these previous findings, this study tests the hypothesis that gp120-IIIB selectively induces apoptosis in CXCR4-expressing androgen-independent prostate cancer cells and tumors.

Materials and Methods

Proteins and Antibodies

gp120-IIIB protein was obtained from Mardx Diagnostics and bovine serum albumin (BSA) was purchased from Sigma. Mouse IgG_{2a} anti-human fusin/CXCR4 and anti-mouse lymphatic endothelial cell marker LYVE-1 monoclonal antibodies were obtained from R&D Systems. Rat anti-mouse CD31, anti-mouse CD34, and anti-human CD44 antibodies were purchased from BD Pharmingen. Anti-active capase-3 and -9 antibodies were obtained from Epitomics and Biovision, respectively.

Cell Lines and Cell Culture

Prostate cancer cell lines (PC3 and DU145) were obtained from the American Type Culture Collection. PrEC cells (Cambrex) were cultured in prostate epithelial basal medium (Cambrex). PC3 cells were cultured in F12K medium with 2.0 mmol/L L-glutamine adjusted to contain 1.5 g/L sodium bicarbonate (American Type Culture Collection) with 10% fetal bovine serum (Sigma) at 37°C and 5% CO_2. DU145 cells were cultured in Eagle's MEM with 10% fetal bovine serum at 37°C and 5% CO_2. Both prostate cancer cell lines were switched to RPMI 1640 (Cellgro) supplemented with 10% fetal bovine serum at 37°C and 5% CO_2 after five passages.

Flow Cytometry Analysis of CXCR4 Expression

PC3, DU145, and PrEC cells were washed three times in PBS supplemented with 0.5% BSA (fluorescence-activated cell sorting buffer) and stained with 1.0 μg isotype control mouse IgG_{2a} or mouse anti-human CXCR4 monoclonal antibodies (R&D Systems) per 10^6 cells for 15 min at room temperature. Cells were washed with 1.0 mL fluorescence-activated cell sorting buffer to remove unbound antibodies. After the final wash, labeled cells were fixed in 500 μL of 2% paraformaldehyde in PBS and 10^5 cells were analyzed by flow cytometry using a FACScan flow cytometer and CellQuest software (BD Pharmingen).

Flow Cytometry Analysis of Apoptosis

Prostate cancer cell lines (PC3 and DU145) and PrEC cells were cultured in 24-well culture plates at a density of 10^5 per well and treated with or without 100 ng/mL gp120-IIIB (Mardx Diagnostics), 1 μg/mL anti-CXCR4 monoclonal antibody, or isotype control antibody IgG_{2a} antibody (R&D Systems) and incubated overnight at 37°C with 5% CO_2. Next, cells were stained using the Vybrant Apoptosis assay (Invitrogen) according to the manufacturer's protocols and assessed by flow cytometry using a FACScan flow cytometer and CellQuest software (BD Pharmingen).

RNA Isolation and mRNA Expression Analysis

Human mRNA sequences of CXCR4, caspase-3, and caspase-9 mRNAs as well as 18S rRNA were obtained from the NIH/National Center for Biotechnology Information gene bank database (accession nos. NM003467, U26943, U60521, and X00686.1, respectively). Primers were designed using the Primer 3 software (Whitehead Institute at Massachusetts Institute of Technology), which generated amplicons 188, 67, 86, and 149 bp in size for CXCR4, caspase-3, and caspase-9 mRNAs and 18S rRNA, respectively. Thermodynamic analysis of the primers was conducted using computer programs: Primer Premier (Integrated DNA Technologies) and Massachusetts Institute of Technology Primer III webware. The resulting primers were compared against the entire human genome using National Center for Biotechnology Information to confirm specificity and insure they flanked mRNA splicing regions. Total RNA was isolated using Tri-reagent (Molecular Research Center) according to the manufacturer's protocols. Potential genomic DNA contamination was removed from these samples by treatment with RNase-free DNase (Invitrogen) for 15 min at 37°C. RNA was then precipitated and resuspended in RNA secure (Ambion). Next, cDNA was generated by reverse transcribing 1.5 μg total RNA using TaqMan reverse transcription reagent (Applied Biosystems) according to the manufacturer's protocols and amplified with specific cDNA primers using SYBR Green PCR master mix reagents (Applied Biosystems). The copies (>10) of target mRNA relative to 18S rRNA copies were evaluated by real-time PCR using the Bio-Rad ICycler and software.

Colorimetric Caspase Assays

PC3 and DU145 cell lines and PrEC cells were seeded in 24-well culture plates (10^6 per well) in complete RPMI 1640. Cells were treated with 100 ng/mL gp120-IIIB or BSA as control. Caspase-3 and -9 activity was tested after 16 h of treatment using active caspase assays (Biovision) according to the manufacturer's protocol. Briefly, cells were harvested and resuspended in chilled lysis buffer, incubated on ice for 10 min, and centrifuged for 10 min at 10,000 × *g*. Supernatants were transferred in fresh tubes and total proteins in cytosolic extracts were estimated by using the Bradford protein assay (Bio-Rad). Protein (200 μg) was diluted in 50 μL cell lysis buffer and 50 μL of 2× reaction buffer containing 10 mmol/L DTT. Next, 5 μL of 4 mmol/L *p*-nitroanilide substrate was added and samples were incubated at 37°C for 2 h and read at 405 nm.

In vivo Tumor Growth

Male severe combined immunodeficient mice (4–6 weeks old) were obtained from Charles River Laboratory. Prostate cancer cells (PC3 and DU145) were counted using a hemacytometer. A sterile, individual syringe for each mouse was prepared and used to subcutaneously inject 2×10^6 cells in 100 μL serum-free RPMI 1640 in the right lateral flank using a 27.5-gauge needle. All mice were monitored daily and tumor growth was monitored twice per week. Once tumors reached ~500 mm^3, mice received intraperitoneal injections of 100 ng gp120-IIIB or BSA in 100 μL PBS every 3 days for 18 days. Tumor size was measured before each treatment using a Thorpe engineer's caliper (Biomedical

Research Instruments). After 18 days of treatment, mice were sacrificed and tumors were excised and fixed for immunohistochemistry analysis.

Immunohistochemical Staining

Paraffin-embedded sections were deparaffinized following three exchanges in xylene for 5 min each, rehydration through a graded series of ethanol for 5 min each (100%, 90%, 70%, and water alone), and finally rinsed in PBS (pH 7.4). Endogenous peroxidase was blocked using 3% H_2O_2 for 5 min and blocked with 3% goat serum for 1 h at room temperature. The sections were incubated overnight at 4°C with rat anti-mouse CD34 (10 μg/mL; BD Pharmingen), anti-human CD44 (10 μg/mL; BD Pharmingen), anti-mouse LYVE-1 (20 μg/mL; R&D Systems), anti-active human caspase-9 (15 μg/mL; Epitomics), and active human caspase-3 (1:50 dilution; Epitomics) antibodies or associated isotype control antibodies in PBS. After washing with PBS, sections were incubated with biotinylated IgG antibody (BD Pharmingen) for 30 min at room temperature and washed with PBS. The sections were incubated with peroxidase-conjugated streptavidin or alkaline phosphatase-conjugated streptavidin (BD Pharmingen) for 30 min in a moist chamber and washed with PBS. The site of peroxidase complex was visualized by diaminobenzidine tetrahydrochloride solution (Biogenex) or alkaline phosphatase with AP New Magenta (Bio-FX Laboratory). Sections were subsequently counterstained with hematoxylin and dehydrated through a graded series of ethanol. After dehydration, the sections were passed through xylene and mounted with paramount (Fisher Scientific). Slides were observed using a Leica DMLB compound microscope with a ×20 objective.

Statistics

Sigma Plot 2000 (Systat Software) was used to compile data. Kolmogorov-Smirnov two-sample test using Cell-Quest Software (BD Pharmingen) for Macintosh computers was used to compute the statistical significance ($P < 0.001$) between PrEC and PC3 or DU145 cell flow cytometry histograms. The Student's *t* test using a two-factor, unpaired test was applied to the significance of differences of other results with $P < 0.01$.

Results

CXCR4 Expression by the Prostate Cancer Cell Lines and PrEC Cells

Prostate cancer cell lines previously isolated from bone (PC3) or brain (DU145) metastases significantly expressed CXCR4 mRNA and surface protein than compared with PrEC cells (Fig. 1). PC3 cells expressed significantly more copies of CXCR4 transcripts than DU145 cells. CXCR4 protein expression by prostate cancer cells and PrEC cells was confirmed by flow cytometry. The cell surface CXCR4 expression by the prostate cancer cell lines was significantly higher than PrEC cells. Moreover, PC3 cells expressed higher levels of CXCR4 than DU145 cells.

gp120-IIIB-Mediated Apoptosis

gp120-IIIB induced apoptosis of prostate cancer cells but not PrEC cells (Fig. 2). PC3 cells, which expressed the highest levels of CXCR4, also displayed the greatest increase in cell permeability and chromatin condensation after gp120-IIIB treatment than compared with DU145 cells. The lower level of chromatin condensation correlated with the lower concentration of CXCR4 expression by DU145 cells relative to PC3 cells. This increase in cell permeability and chromatin condensation after gp120-IIIB treatment was significantly reduced by CXCR4 blockade. Interestingly, gp120-IIIB treatment significantly enhanced active caspase-3 and -9 expression by PC3 and DU145 cell lines than compared with PrEC

cells, which was also reduced by CXCR4 blockade (Fig. 3). These data show that gp120-IIIB-mediated apoptosis of prostate cancer cells occurs in CXCR4-dependent fashion.

Effect of gp120-IIIB Treatment on Tumor-Associated Endothelium Development Tumor Growth

Tumor-bearing mice were treated with gp120-IIIB or BSA (controls) every 3 days for 18 days. Treatment using gp120-IIIB yielded significant decreases in the size of PC3 and DU145 tumors than compared with control mice (Fig. 4). We further investigated the effect of gp120-IIIB on human CD44, active caspase-3, and active caspase-9 as well as murine CD34 and LYVE-1 expression by PC3 tumors. Tumors excised from the mice receiving gp120-IIIB showed higher expression of active caspase-3 and -9 than tumors from control mice (Fig. 5). This increase in caspase activity correlated with lower LYVE-1 but not CD34 expression than compared with tumors excised from control mice (Fig. 6). Taken together, the reduction in the tumor size of mice treated with gp120-IIIB was associated with enhanced caspase-3 and -9 activity as well as lower levels of lymphangiogenesis and adhesion biomarkers.

Discussion

Prostate cancer is one of the leading causes of cancer-related mortalities among men in United States. CXCR4 has been recently implicated in prostate cancer metastasis (1, 2). CXCR4 also acts as a coreceptor for gp120-IIIB, which is a glycoprotein expressed by HIV-1 (12, 13, 21). In this study, the cytotoxic effects of gp120-IIIB were examined using hormone-refractory prostate cancer cell lines (PC3 and DU145) as well as PrEC cells that differentially express CXCR4. For the first time, we have shown that the CXCR4-tropic gp120-IIIB selectively induced apoptosis of prostate cancer cells in a CXCR4-dependent fashion. The amount of apoptosis induced by CXCR4-expressing gp120-IIIB-treated carcinoma cells appeared to be directly proportional to the relative amount of CXCR4 expressed by these cells. Indeed, gp120-IIIB-mediated apoptosis did not occur in PrEC cells, which express lower levels of CXCR4. It is also possible that these significantly slower growing cells may not be susceptible to CXCR4/gp120-IIIB-mediated apoptosis. In confirmation, others have shown that immune and endothelial cells undergo apoptosis via gp120-IIIB-CXCR4 interactions (14, 15), which supports our current findings.

Apoptosis is coordinated by a family of cysteine proteases, which are activated by frequently divergent proapoptotic stimuli (22). Activation of the caspase cascade has been correlated with the onset of apoptosis (23). Caspases are synthesized as relatively inactive precursors that require proteolytic processing for activation (24). The absence of caspase-9 can prevent caspase-3 activation and cytochrome *c*-dependent processing of procaspase-3, which fails to occur in cytosolic extracts of caspase-9 deficient cells (25). Hence, caspase-9 is a critical upstream activator of caspase-3 (26). Once caspase-3 is activated, downstream cell death substrates are cleaved by this enzyme (27). Caspase-3 also amplifies other cell death cascades, including cytochrome *c* release from mitochondria, by cleaving Bcl-2 and converting it from an antiapoptotic to a proapoptotic protein (28). In this study, we have shown that gp120-IIIB caused a significant increase in both initiator (caspase-9) and effector (caspase-3) caspases in a CXCR4-dependent fashion.

In correlation with the differential CXCR4 expression levels of PC3 > DU145 cells, gp120-IIIB induced higher membrane permeability and chromatin condensation in PC3 cells than compared with DU145 cells. These levels might also be attributed to differences in the apoptosis machinery of PC3 and DU145 cell lines. For example, apoptotic DU145 cells, which are Bax deficient, display less chromatin condensation than compared with Bax-positive cancer cells (e.g., PC3 cells; ref. 29). Despite these differences, gp120-IIIB

treatment inhibited PC3 and DU145 xenograft tumor growth at the same rate. Moreover, gp120-IIIB treatment also reduced CD44 expression by tumors in severe combined immunodeficient mice. To this end, tumor progression is regulated by cell-cell and cell-extracellular matrix interactions (30, 31). CD44 is a cell surface receptor for hyaluronan, which is a critical component of the extracellular matrix (32, 33). Hyaluronan and CD44 are often up-regulated at sites of morphogenesis, inflammation, and tumor invasion (34, 35) and play important roles in tumor invasion, growth, and metastasis (36, 37). Studies have shown that CD44 expression by tumors promoted cancer cell survival (38); CD44 also anchors matrix metalloproteinase-9 on the cell surface (39) and works together with transforming growth factor-β1 to promote tumor growth (37). These studies support our findings that gp120-IIIB is capable of lowering tumor progression and CD44 expression by prostate tumor cells. Together, these events increase apoptosis, reduce adherence, and inhibit cell survival and/or growth.

No doubt, angiogenesis and/or lymphangiogenesis are considered hallmarks of prostate cancer progression (40–43). It has also been shown that vascular endothelium are $CD34^+$ (44), whereas lymphatic endothelium express LYVE-1 (45). Although hematogenous metastasis via blood vessels is well recognized for many tumors and correlates with cancer progression (16), it is thought that high interstitial pressure inside tumors prevents the growth of lymphatic vessels into the tumor mass (46). However, recent experimental and clinical data (18–20) strongly indicate that the number and size of lymphatics in and around a tumor is an important determinant of tumor aggressiveness. In light of these reports, we investigated LYVE-1 and CD34 expression by prostate tumors from mice treated with or without gp120-IIIB. Whereas CD34 expression was not affected by gp120-IIIB treatment, the number of LYVE-1-expressing cells was significantly lowered. These data suggest that lymphatic endothelial cell reduction, but not neovascular cell growth inhibition, contributed to the observed reduction in tumor volume following gp120-IIIB treatment. Hence, our findings suggest that gp120-IIIB impedes tumor progression by predominately inhibiting lymphangiogenesis.

In summary, we have shown that gp120-IIIB induced caspase-driven apoptosis of prostate cancer cells but not PrEC cells in a CXCR4-dependent fashion. Further, gp120-IIIB and CXCR4 interaction inhibited tumor growth, which is associated by increased active caspase-3/9 and lower CD44 expression by cancer cells as well as a reduction in the number of LYVE-1-expressing (lymphatic endothelial) cells. Additional studies will be required to dissect the precise molecular mechanisms and interactions between gp120-IIIB and CXCR4 for targeted prostate cancer cell death and reduced tumor-associated lymphangiogenesis. Due to the potential systemic adverse events (14, 15), it may not be feasible to use recombinant gp120-IIIB as a cancer therapeutic. However, this study provides biological and physiologic rationales to develop gp120-IIIB small-molecule or peptide mimics with extended bioavailabilities and tumor specificities that can efficiently target and kill $CXCR4^+$ prostate tumors.

References

1. Taichman RS, Cooper C, Keller ET, Pienta KJ, Taichman NS, McCauley LK. Use of the stromal cell-derived factor-1/CXCR4 pathway in prostate cancer metastasis to bone. Cancer Res. 2002; 62:1832–1837. [PubMed: 11912162]
2. Singh S, Singh UP, Grizzle WE, Lillard JW. CXCL12-4 interactions modulates prostate cancer cell migration, metalloproteinase expression and invasion. Lab Invest. 2004; 84:1666–1676. [PubMed: 15467730]
3. Scala S, Ottaiano A, Ascierto PA, et al. Expression of CXCR4 predicts poor prognosis in patients with malignant melanoma. Clin Cancer Res. 2005; 11:1835–1841. [PubMed: 15756007]

4. Perissinotto E, Cavalloni G, Leone F, et al. Involvement of chemokine receptor 4/stromal cell-derived factor 1 system during osteosarcoma tumor progression. Clin Cancer Res. 2005; 11:490–497. [PubMed: 15701832]
5. Spano JP, Andre F, Morat L, et al. Chemokine receptor CXCR4 and early-stage non-small cell lung cancer: pattern of expression and correlation with outcome. Ann Oncol. 2004; 15:613–617. [PubMed: 15033669]
6. Delilbasi CB, Okura M, Iida S, Kogo M. Investigation of CXCR4 in squamous cell carcinoma of the tongue. Oral Oncol. 2004; 40:154–157. [PubMed: 14693238]
7. Arya M, Patel HR, McGurk C, et al. The importance of the CXCL12-4 chemokine ligand-receptor interaction in prostate cancer metastasis. J Exp Ther Oncol. 2004; 4:291–303. [PubMed: 15844659]
8. Hart CA, Brown M, Bagley S, Sharrard M, Clarke NW. Invasive characteristics of human prostatic epithelial cells: understanding the metastatic process. Br J Cancer. 2005; 92:503–512. [PubMed: 15668715]
9. Phillips RJ, Burdick MD, Lutz M, Belperio JA, Keane MP, Strieter RM. The stromal derived factor-1/CXCL12-CXC chemokine receptor 4 biological axis in non-small cell lung cancer metastases. Am J Respir Crit Care Med. 2003; 167:1676–1686. [PubMed: 12626353]
10. Calandra G, McCarty J, McGuirk J, et al. AMD3100 plus G-CSF can successfully mobilize $CD34^+$ cells from non-Hodgkin's lymphoma, Hodgkin's disease and multiple myeloma patients previously failing mobilization with chemotherapy and/or cytokine treatment: compassionate use data. Bone Marrow Transplant. 2008; 41:331–338. [PubMed: 17994119]
11. Bredeek UF, Harbour MJ. CCR5 antagonists in the treatment of treatment-naive patients infected with CCR5 tropic HIV-1. Eur J Med Res. 2007; 12:427–434. [PubMed: 17933724]
12. Deng H, Liu R, Ellmeier W, et al. Identification of a major co-receptor for primary isolates of HIV-1. Nature. 1996; 381:661–666. [PubMed: 8649511]
13. Feng Y, Broder CC, Kennedy PE, Berger EA. HIV-1 entry cofactor: functional cDNA cloning of a seven-transmembrane, G protein-coupled receptor. Science. 1996; 272:872–877. [PubMed: 8629022]
14. Herbein G, Mahlknecht U, Batliwalla F, et al. Apoptosis of $CD8^+$ T cells is mediated by macrophages through interaction of HIV gp120 with chemokine receptor CXCR4. Nature. 1998; 395:189–194. [PubMed: 9744279]
15. Berndt C, Mopps B, Angermuller S, Gierschik P, Krammer PH. CXCR4 and CD4 mediate a rapid CD95-independent cell death in CD4(+) T cells. Proc Natl Acad Sci U S A. 1998; 95:12556–12561. [PubMed: 9770524]
16. Dachs GU, Tozer GM. Hypoxia modulated gene expression: angiogenesis, metastasis and therapeutic exploitation. Eur J Cancer. 2000; 36:1649–1660. [PubMed: 10959051]
17. Plate KH. From angiogenesis to lymphangiogenesis. Nat Med. 2001; 7:151–152. [PubMed: 11175837]
18. Fukuda H, Yamada T, Kamata S, Saitoh H. Anatomic distribution of intraprostatic lymphatics: implications for the lymphatic spread of prostate cancer—a preliminary study. Prostate. 2000; 44:322–327. [PubMed: 10951497]
19. Skobe M, Hawighorst T, Jackson DG, et al. Induction of tumor lymphangiogenesis by VEGF-C promotes breast cancer metastasis. Nat Med. 2001; 7:192–198. [PubMed: 11175850]
20. Stacker SA, Caesar C, Baldwin ME, et al. VEGF-D promotes the metastatic spread of tumor cells via the lymphatics. Nat Med. 2001; 7:186–191. [PubMed: 11175849]
21. Littman DR. Chemokine receptors: keys to AIDS pathogenesis? Cell. 1998; 93:677–680. [PubMed: 9630212]
22. Thornberry NA, Lazebnik Y. Caspases: enemies within. Science. 1998; 281:1312–1316. [PubMed: 9721091]
23. Bowen C, Voeller HJ, Kikly K, Gelmann EP. Synthesis of procaspases-3 and -7 during apoptosis in prostate cancer cells. Cell Death Differ. 1999; 6:394–401. [PubMed: 10381629]
24. Stennicke HR, Salvesen GS. Catalytic properties of the caspases. Cell Death Differ. 1999; 6:1054–1059. [PubMed: 10578173]
25. Kuida K, Haydar TF, Kuan CY, et al. Reduced apoptosis and cytochrome *c*-mediated caspase activation in mice lacking caspase 9. Cell. 1998; 94:325–337. [PubMed: 9708735]

26. Hakem R, Hakem A, Duncan GS, et al. Differential requirement for caspase 9 in apoptotic pathways *in vivo*. Cell. 1998; 94:339–352. [PubMed: 9708736]
27. Reed JC. Cytochrome *c*: can't live with it-can't live without it. Cell. 1997; 91:559–562. [PubMed: 9393848]
28. Cheng EH, Kirsch DG, Clem RJ, et al. Conversion of Bcl-2 to a Bax-like death effector by caspases. Science. 1997; 278:1966–1968. [PubMed: 9395403]
29. Kessel D, Vicente MGH, Reiners JJ Jr. Initiation of apoptosis and autophagy by photodynamic therapy. Lasers Surg Med. 2006; 38:482–488. [PubMed: 16615135]
30. Liotta LA. Tumor invasion and metastases—role of the extracellular matrix: Rhoads Memorial Award Lecture. Cancer Res. 1986; 46:1–7. [PubMed: 2998604]
31. Hynes RO. Cell adhesion: old and new questions. Trends Cell Biol. 1999; 9:M33–M37. [PubMed: 10611678]
32. Stamenkovic I, Amiot M, Pesando JM, Seed B. A lymphocyte molecule implicated in lymph node homing is a member of the cartilage link protein family. Cell. 1989; 56:1057–1062. [PubMed: 2466575]
33. Aruffo A, Kolanus W, Bevilacqua M, Seed B. CD44 is the principal cell surface receptor for hyaluronate. Science. 1990; 250:1132–1135. [PubMed: 1701275]
34. Knudson W, Biswas C, Toole BP. Interactions between human tumor cells and fibroblasts stimulate hyaluronate synthesis. Proc Natl Acad Sci U S A. 1984; 81:6767–6771. [PubMed: 6593727]
35. Yeo TK, Nagy JA, Yeo KT, Dvorak HF, Toole BP. Increased hyaluronan at sites of attachment to mesentery by CD44-positive mouse ovarian and breast tumor cells. Am J Pathol. 1996; 148:1733–1740. [PubMed: 8669459]
36. Gunthert U, Hofmann M, Rudy W, et al. A new variant of glycoprotein CD44 confers metastatic potential to rat carcinoma cells. Cell. 1991; 65:13–24. [PubMed: 1707342]
37. Yu Q, Stamenkovic I. Cell surface-localized matrix metalloproteinase-9 proteolytically activates TGF-β and promotes tumor invasion and angiogenesis. Genes Dev. 2000; 14:163–176. [PubMed: 10652271]
38. Yu Q, Toole BP, Stamenkovic I. Induction of apoptosis of metastatic mammary carcinoma cells *in vivo* by disruption of tumor cell surface CD44 function. J Exp Med. 1997; 186:1985–1996. [PubMed: 9396767]
39. Yu Q, Stamenkovic I. Localization of matrix metalloproteinase 9 to the cell surface provides a mechanism for CD44-mediated tumor invasion. Genes Dev. 1999; 13:35–48. [PubMed: 9887098]
40. Weidner N, Carroll PR, Flax J, Blumenfeld W, Folkman J. Tumor angiogenesis correlates with metastasis in invasive prostate carcinoma. Am J Pathol. 1993; 143:401–409. [PubMed: 7688183]
41. Bettencourt MC, Bauer JJ, Sesterhenn IA, Connelly RR, Moul JW. CD34 immunohistochemical assessment of angiogenesis as a prognostic marker for prostate cancer recurrence after radical prostatectomy. J Urol. 1998; 160:459–465. [PubMed: 9679898]
42. Brawer MK, Deering RE, Brown M, Preston SD, Bigler SA. Predictors of pathologic stage in prostatic carcinoma. The role of neovascularity. Cancer. 1994; 73:678–687. [PubMed: 7507798]
43. Barth PJ, Weingartner K, Kohler HH, Bittinger A. Assessment of the vascularization in prostatic carcinoma: a morphometric investigation. Hum Pathol. 1996; 27:1306–1310. [PubMed: 8958303]
44. Podgrabinska S, Braun P, Velasco P, Kloos B, Pepper MS, Skobe M. Molecular characterization of lymphatic endothelial cells. Proc Natl Acad Sci U S A. 2002; 99:16069–16074. [PubMed: 12446836]
45. Banerji S, Ni J, Wang SX, et al. LYVE-1, a new homologue of the CD44 glycoprotein, is a lymph-specific receptor for hyaluronan. J Cell Biol. 1999; 144:789–801. [PubMed: 10037799]
46. Carmeliet P, Jain RK. Angiogenesis in cancer and other diseases. Nat Med. 2000; 6:1102–1103. [PubMed: 11017137]

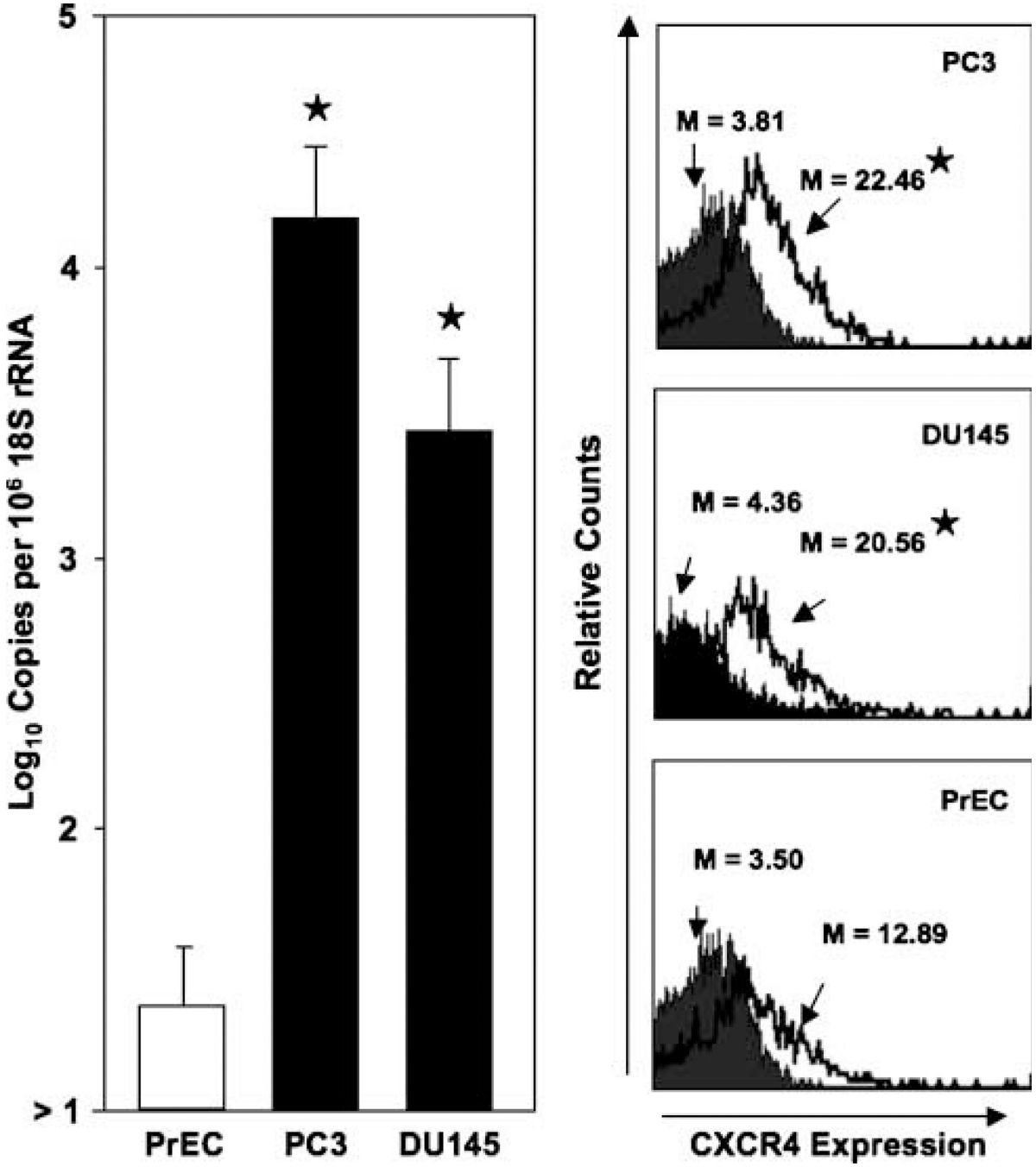

Figure 1.

CXCR4 expressed by prostate cancer cell lines and PrEC cells. Total RNA was isolated from prostate cancer cell lines and PrEC cells and quantitative real-time PCR analysis of CXCR4 mRNA expression was done in triplicate. Copies of transcripts were expressed relative to actual copies of 18S rRNA ± SE. PC3 and DU145 cell lines and PrEC cells were stained with PE-conjugated anti-CXCR4 (*open histogram*) or PE-conjugated isotype control antibodies (*solid histogram*) and quantified in triplicate by flow cytometry. *M,* mean fluorescent intensities of CXCR4-positive cells. ★, $P < 0.001$, statistical significance between normal and prostate cancer cell lines.

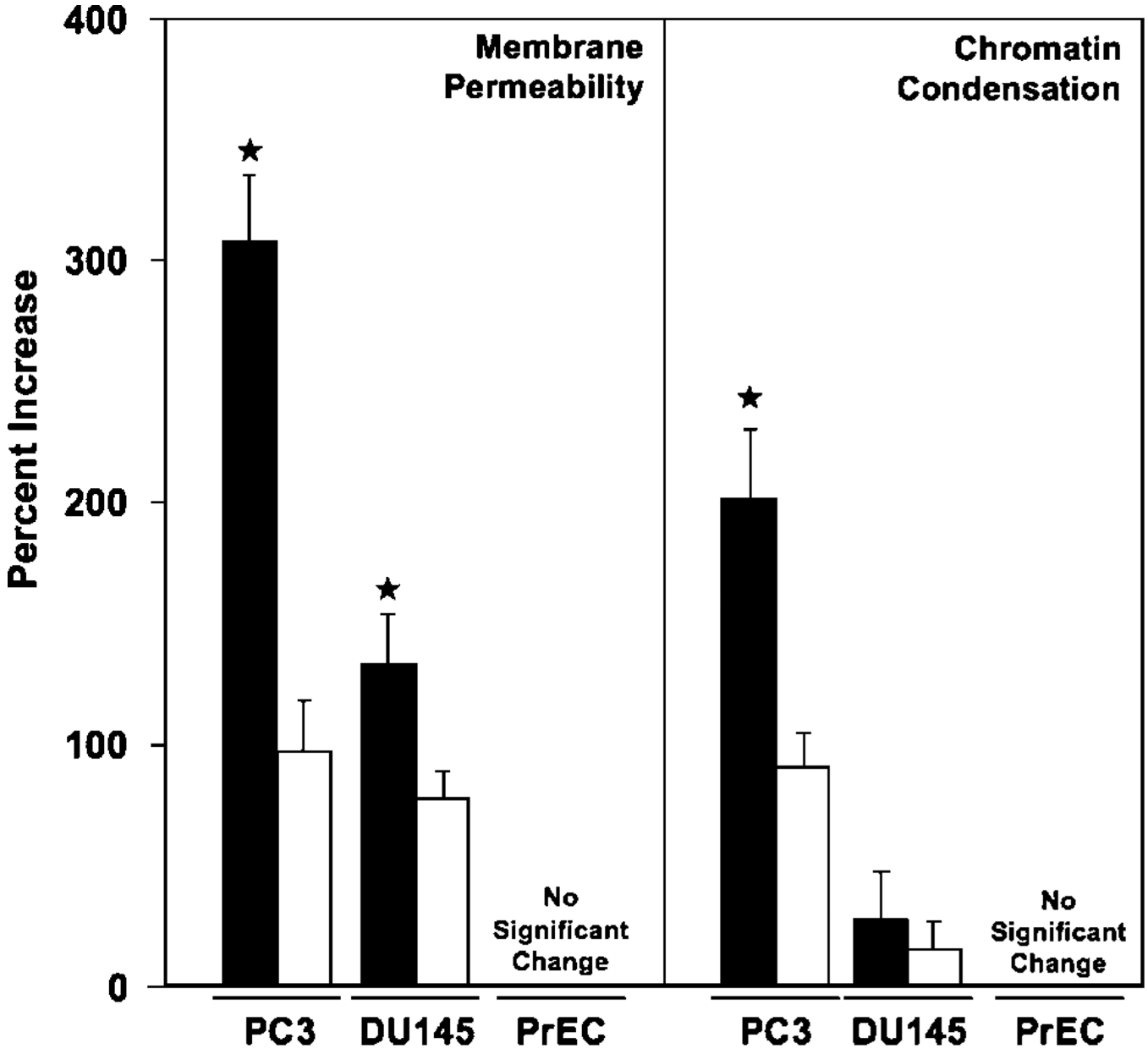

Figure 2.

gp120-IIIB-induced apoptosis. PC3 and DU145 cell lines and PrEC cells were treated with 100 ng/mL gp120-IIIB (*solid columns*) or 100 ng/mL gp120-IIIB + 1 μg/mL anti-CXCR4 antibody (*open columns*) in 100 μL PBS and incubated in 5% CO_2 overnight (16 h). The percent increase in the number of membrane-permeable cells or cells undergoing chromatin condensation compared with untreated controls was measured by flow cytometry that was done in triplicate in three separate experiments. ★, $P < 0.01$, statistical significance in the percent increase of apoptotic cells after gp120-IIIB treatment or decrease in cell permeability or chromatin condensation between cells treated with gp120-IIIB and cells treated with gp120-IIIB + anti-CXCR4 antibody.

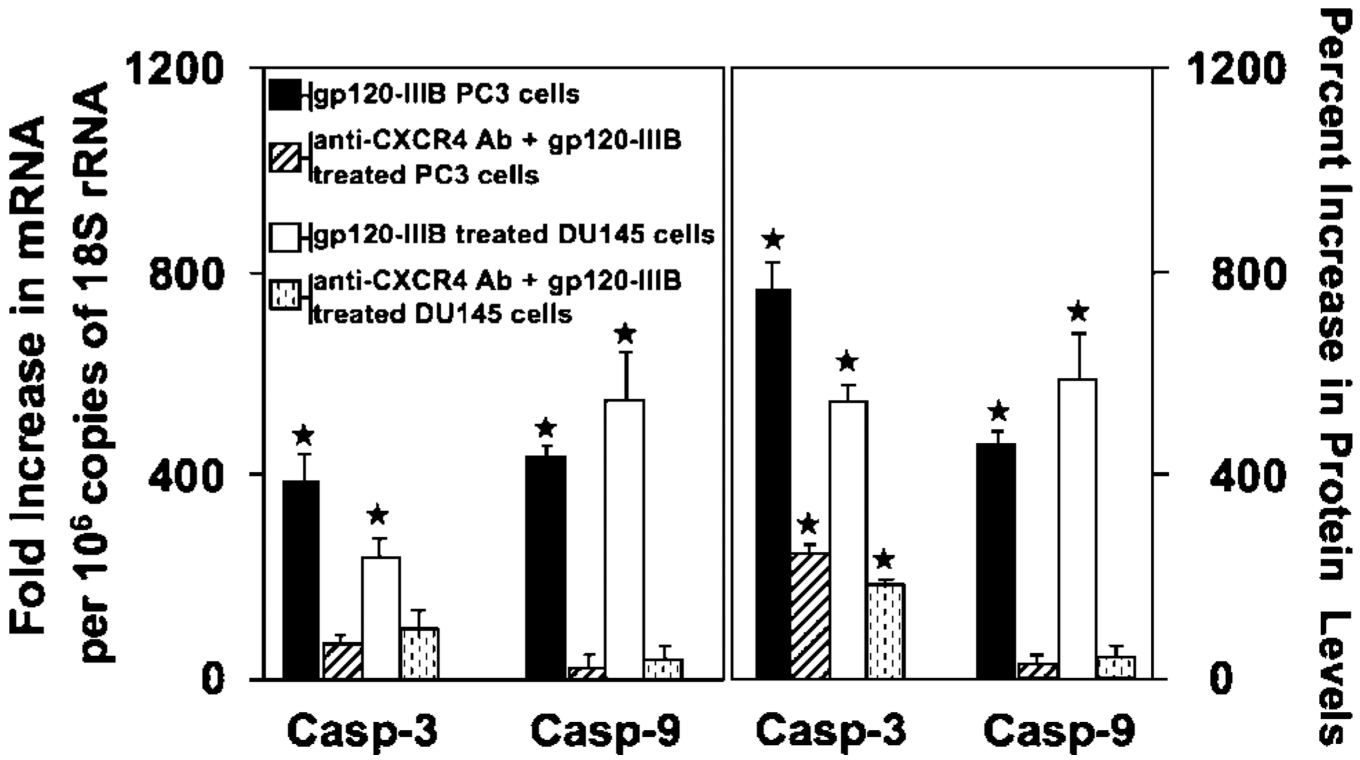

Figure 3.

gp120-IIIB-induced caspase-3 and -9 expression. PC3 and DU145 cells were treated with 100 ng/mL gp120-IIIB or 100 ng/mL gp120-IIIB + 1 μg/mL anti-CXCR4 antibody. Total RNA was isolated 16 h after treatment and proteins were isolated after 24 h of treatment. Caspase mRNA was quantified by quantitative real-time PCR and active caspase protein was confirmed by ELISA. ★, $P < 0.01$, statistical significance in the increase of caspase(s) mRNA or active protein expression following gp120-IIIB treatment compared with controls.

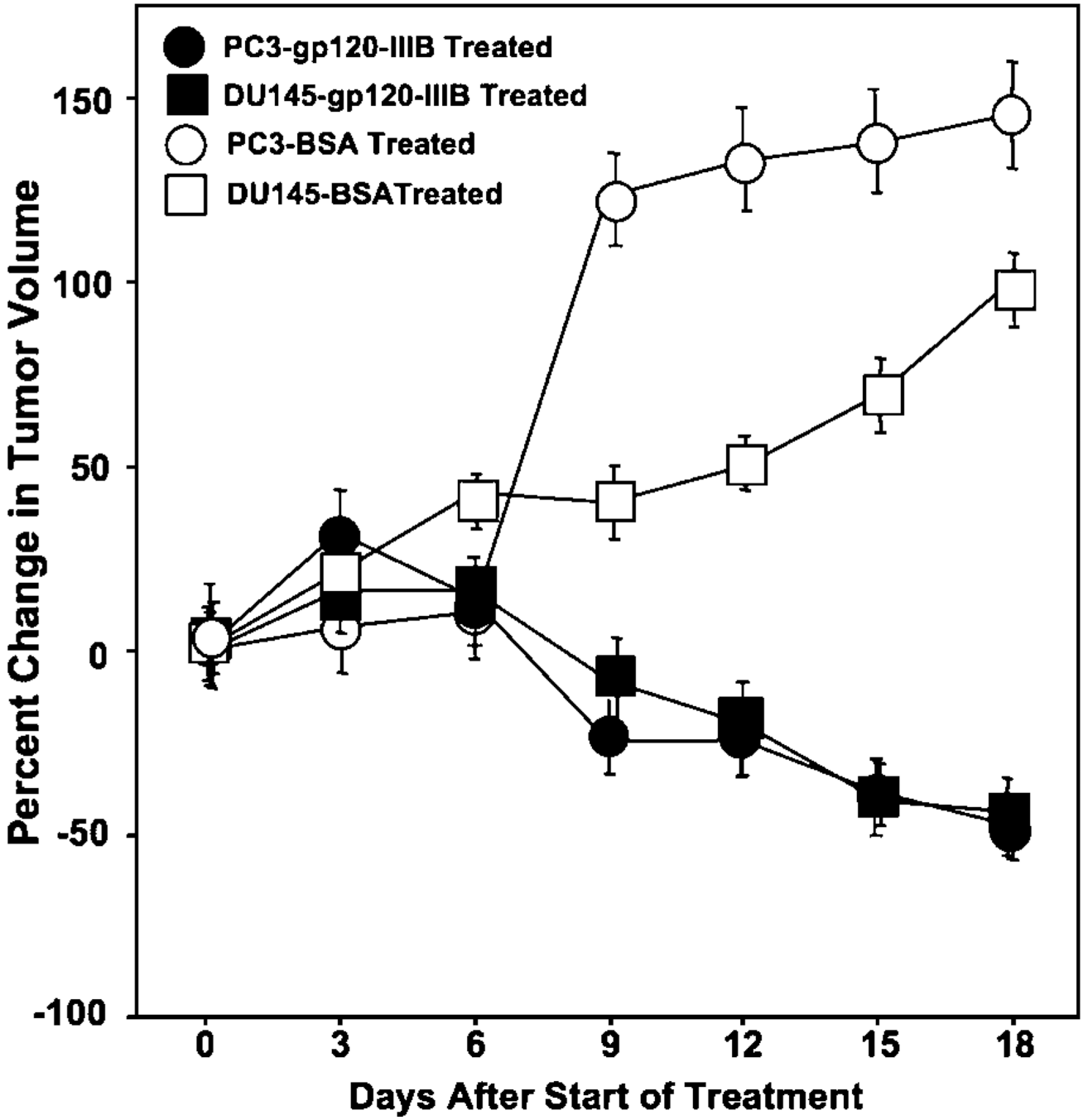

Figure 4.

Effects of gp120-IIIB treatment on prostate tumor growth. Male severe combined immunodeficient mice were subcutaneously challenged in the right bilateral flank with 2×10^6 PC3 or DU145 cells in 100 μL serum-free RPMI 1640. Tumors were allowed to reach 500 mm^3 in size. Subsequently, tumor-bearing mice received 100 ng/mL gp120-IIIB in PBS or 100 ng/mL BSA in PBS by intraperitoneal injection every 3 d. Mean ± SE percentage change in tumor size from day 0 was measured using a Thorpe engineer's caliper from three separate experiments with experimental groups containing five mice each. ★, $P < 0.01$, statistical significance between gp120-IIIB-treated and control groups.

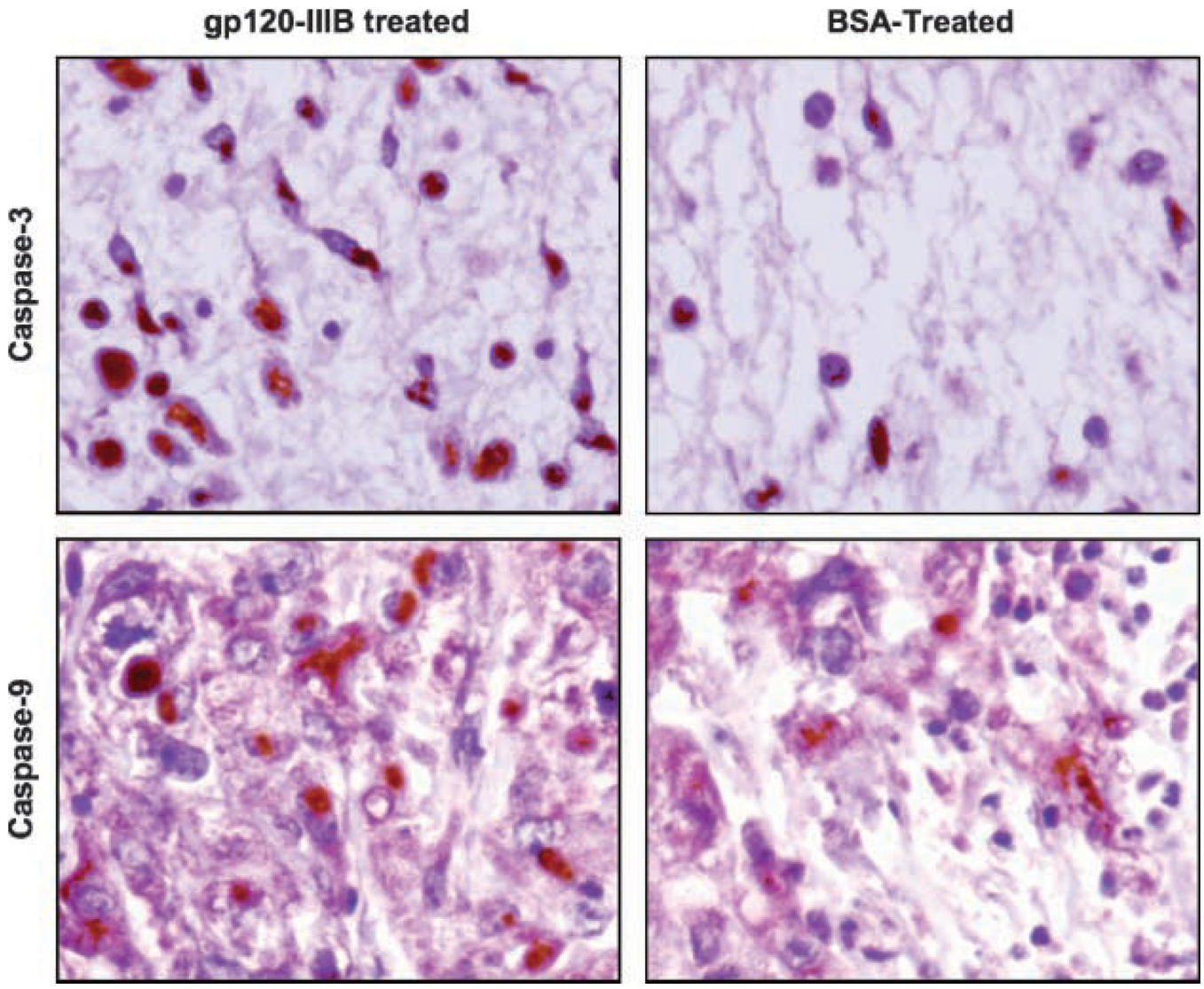

Figure 5.

Active caspase-3 and -9 expression by prostate tumors. Sections from PC3 tumors were excised from mice treated with gp120-IIIB or BSA, stained for active caspase-3 or -9, and counterstained with hematoxylin. Representative sections from three separate experiments (×20 magnification), with groups containing five mice each.

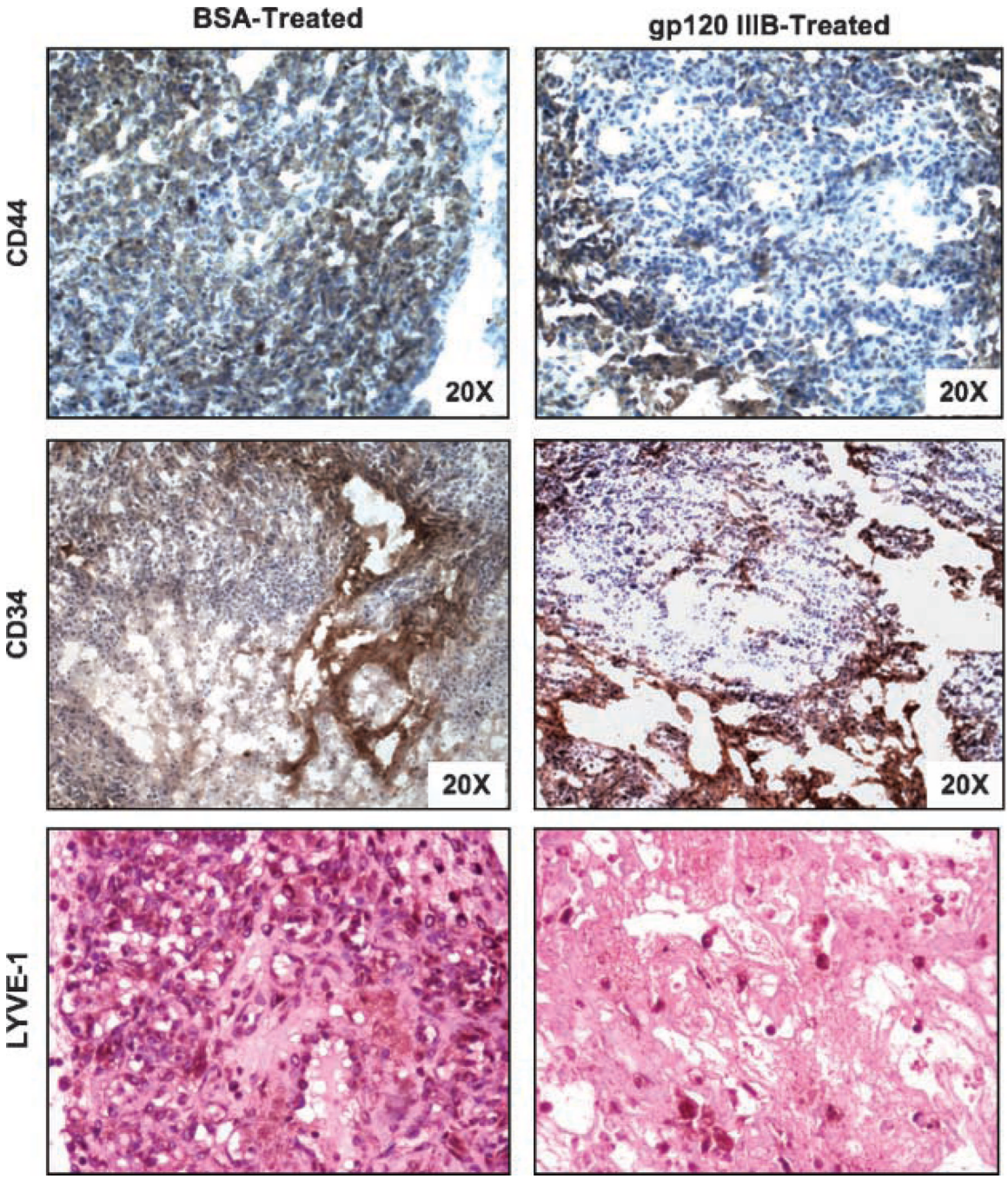

Figure 6.
Expression of CD44, LYVE-1, and CD34 by prostate tumors. Sections from PC3 tumors were excised from mice following gp120-IIIB treatment, stained for CD44, LYVE-1, or CD34 expression, and counterstained with hematoxylin. Representative sections from three separate experiments (×20 magnification), with groups containing five mice each.